



Arsenic(III) adsorption from aqueous solutions on novel carbon cryogel/ceria nanocomposite

Tamara Minović Arsić¹, Ana Kalijadis¹, Branko Matović¹, Milovan Stoiljković¹, Jelena Pantić¹, Jovan Jovanović², Rada Petrović², Bojan Jokić², Biljana Babić^{1,*}

¹Vinča Institute of Nuclear Sciences, University of Belgrade, P.O. Box 522, 11000 Belgrade, Serbia

²Faculty of Technology and Metallurgy, University of Belgrade, Karnegijeva 4, 11000 Belgrade, Serbia

Received 2 February 2016; Received in revised form 1 March 2016; Accepted 7 March 2016

Abstract

Carbon cryogel/ceria composite, with 10 wt.% of ceria, was synthesized by mixing of ceria and carbon cryogel (CC). The sample was characterized by field emission scanning electron microscopy, nitrogen adsorption and X-ray diffraction. The adsorption of arsenic(III) ions from aqueous solutions on carbon cryogel/ceria nanocomposite was studied as a function of time, solution pH and As(III) ion concentration. The results are correlated with previous investigations of adsorption mechanism of arsenic(III) on carbon cryogel. Adsorption dose experiments showed that the mass of the adsorbent was reduced for 20 times, in comparison with pure CC, for the same amount of adsorbed arsenic(III) ions. BET isotherm was used to interpret the experimental data for modelling liquid phase adsorption.

Keywords: carbon cryogel/ceria composite, adsorption, arsenic (III)

I. Introduction

Arsenic water pollution is widespread world problem. High arsenic concentrations in drinking and irrigation water have been measured in large areas of Bangladesh, India, China, and in some parts of United States of America, Argentina, Australia, Chile, Mexico, Taiwan, Vietnam and Thailand [1]. More than 100 million people are at risk for consuming water with arsenic level above 0.01 ppm [2].

Arsenic is highly toxic element. There are numerous studies focused on health effects of chronic arsenic exposure [3–6]. It has been found that consuming water with elevated level of arsenic leads to pigmentation and keratosis of the skin, chronic pulmonary disease, diabetes, miscarriage, abortion, infant mortality, vascular disease, cancers of the skin, lung, liver and urinary tract. Due to the sufficient evidence, arsenic and its inorganic compounds have been classified as Group I carcinogens to humans [7]. Hence, it has to be removed from drinking water. Various techniques are being used for reducing arsenic concentration: reverse osmosis, activated alumina, coagulation/filtration, ion exchange, electro-

dialysis, and oxidation/filtration [8]. Singh *et al.* [2] gave a critical review of remediation techniques for arsenic.

Among all methods proposed for arsenic removal adsorption stands out as a simple and efficient method. A wide range of sorbent materials can be used to decrease arsenic concentration in water solutions, such as thiol-functionalized chitin nanofibres, goethite-based adsorbent, zero valent iron, synthetic siderite, titanium dioxide and many others [9–13]. Ungureanu *et al.* [14] gave a review of latest advances in adsorption of arsenic.

In our previous study we showed that carbon cryogel (CC) can be used as As(III) adsorbent over a wide pH range [15]. Based on the experimental data, conclusions were brought that the surface of adsorbent should be high and neutral, i.e. the amount of surface functional groups should be reduced to increase the arsenic adsorption capacity. For that purpose we synthesized carbon cryogel/ceria nanocomposite with 10 wt.% of ceria, assuming that the novel material would have better arsenic adsorption capacity comparing to the pure carbon cryogel.

The aim of this study is to investigate As(III) adsorption process on carbon cryogel/ceria composite. Adsorption kinetic, the effect of solution pH and arsenic concentration on removal rate were examined in

*Corresponding author: tel: +381113408224, e-mail: babicb@vinca.rs

batch system. Adsorption kinetics, as well as adsorption isotherms, were fitted to several theoretical models.

II. Experimental

2.1. Chemicals and materials

Resorcinol ($C_6H_4(OH)_2$, 99% purity, Merck), formaldehyde (HCHO, 36% methanol stabilized, Fluka Chemie) and sodium carbonate (Na_2CO_3 , p.a. quality, Merck) were used for the synthesis of carbon cryogel. Cerium nitrate ($Ce(NO_3)_3$) (Aldrich, USA) and NaOH (p.a. Zorka, Serbia) were used as starting materials for synthesis of ceria.

Sodium arsenite ($NaAsO_2$, analytical reagent, Mallinckrodt) was used to prepare arsenic(III) stock solution. As(III) solutions used in batch experiments were obtained by diluting the As(III) stock solution to desired concentrations with distilled water.

2.2. Composite synthesis

Carbon cryogel was synthesized by the method previously described by Babic *et al.* [15,16]. Briefly, it is a polycondensation reaction of resorcinol with formaldehyde in water solution with sodium carbonate as a basic catalyst, followed by freeze-drying and carbonization in inert atmosphere at 800 °C. Very important step prior to drying is rinsing of gel in *t*-butanol ($C_4H_{10}O$, 99.5% for analysis, Acros Organics, USA) so that water solvent could be replaced with organic one which does not exhibit significant changes in the volume of molecules during the freezing process.

Ceria was synthesized by a self-propagating room temperature method previously in detail described by Matović *et al.* [17]. Calculated masses of reactants were vigorously hand mixed in alumina mortar with alumina pestle for about 5 minutes and left in air for 2 hours. Then, the reaction product mixture was rinsed in centrifuge Centurion 1020D at 350 rpm to remove $NaNO_3$.

Carbon cryogel/ceria composite was synthesized by mixing of ceria and CC in mortar for about 15 minutes. The nominal CeO_2 loading was 10 wt.%. Since there is no literature data about carbon cryogel/ceria composite, we have assumed that 10 wt.% of ceria would be enough to reduce the amount of the functional groups on surface of CC and, at the same time, not to significantly decrease the CC's surface area. Our assumption was based on several facts. CC is carbon material with high specific surface area and turbostratic structure, i.e. a large number of unpaired electrons exist on the surface [18]. On the other side, in our previous investigations we confirmed the presence of the Ce^{3+} and O^{2-} vacancies in the structure of the ceria obtained by the SPRT method [17]. Due to that, we have concluded that this non-stoichiometric ceria can be the source of the electrons. From the economical point of view, the prices of CC's precursors are significantly lower in comparison with ceria precursor and, consequently, the amount of ceria should be as low as possible.

2.3. Composite characterization

The surface morphology of the carbon cryogel/ceria composite was observed using a field emission scanning electron microscope (FESEM) TESCAN Mira3 XMU at 20 kV.

The specific surface area and median pore size of the carbon cryogel/ceria composite were analysed using the Surfer (Thermo Fisher Scientific, USA).

The carbon cryogel/ceria composite sample was characterized by recording their powder X-ray diffraction (XRD) pattern on a Rigaku diffractometer model Ultima IV using $Cu K\alpha$ radiation with a Ni filter. Angular 2θ -region between 10 and 80° was explored at a scan rate of 1°/s with the angular resolution of 0.02°.

2.4. Batch adsorption experiments

All adsorption experiments were carried out at room temperature (20 ± 2 °C) in a set of closed 50 ml PVC bottles using a mechanical shaker at a rate of 60 cycles/min.

In the adsorption kinetic study the initial As(III) concentration was $C_0 = 10$ mg/l and no pH adjustment was taken. We added 0.1 g of composite material into 25 ml of As(III) aqueous solution. Time intervals were varied from 10 min to 24 h. After continuous shaking for predetermined period, the solid was separated by filtration, and the remaining As(III) concentration was measured using atomic absorption spectroscopy - hydride generation technique.

To study the effect of pH on adsorption, 25 ml of As(III) aqueous solution of initial concentration $C_0 = 10$ mg/l was continuously shaken with 0.1 g of the carbon cryogel/ceria composite for 24 h, at different pH values. To adjust the pH to 2–11, 0.1 M HNO_3 and 0.1 M KOH were used. After continuous stirring for predetermined time interval, the solid was separated by filtration and arsenic concentration in the remaining solution was determined.

Adsorbent dose study was conducted in order to determine the optimal mass of adsorbent in regard to arsenic removal percentage. We added different masses of composite material ($m = 10$ –100 mg) into 25 ml of As(III) aqueous solution, $C_0 = 10$ mg/l, at native pH. After continuous stirring for 24 h, the solid was separated by filtration and arsenic concentration in the remaining solution was measured.

Adsorption isotherms were studied by varying initial concentration of As(III) from 0.25–14 mg/l. Solutions with specific concentrations of As(III) were prepared by dissolving of arsenic stock solution into distilled water. Then, 5 mg of the synthesized carbon cryogel/ceria composite was added to 25 ml of the solution under stirring for 24 h. The pH value was adjusted to 5, 7 and 9 by (0.1 M) HNO_3 and KOH. At the end of pre-selected equilibrium time, the solid was separated by filtration and arsenic concentration in the remaining solution was determined.



Figure 1. FESEM image of carbon cryogel/ceria composite

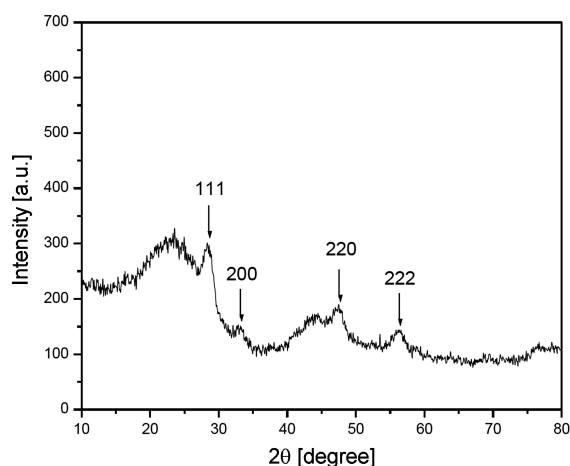


Figure 2. Room temperature XRD of carbon cryogel/ceria composite

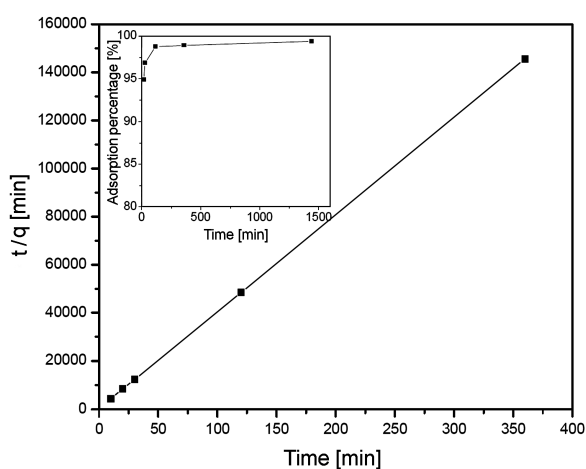


Figure 3. The best fit of the pseudo-second order kinetic equation. Inset: Adsorption kinetic of As(III) on carbon cryogel/ceria composite; $C_0 = 10$ mg/l, $V = 25$ ml, $m = 100$ mg, $pH = 5$

III. Results and discussion

3.1. Structural characterization

FESEM image, presenting the morphology and texture of the carbon cryogel/ceria composite, is shown at Fig. 1. It is evident that presence of 10 wt.% of ceria significantly changed the surface morphology in comparison with the pure CC whose structure is shown in our previous paper [15]. The morphology of the carbon cryogel/ceria composite, i.e. the distribution of ceria in CC is very homogeneous. Nanoparticles of ceria have penetrated into the larger carbon cryogel's pores and, consequently, the pore radius decreased. This conclusion was confirmed by nitrogen adsorption-desorption measurements (Table 1). The results indicate that overall specific surface area, S_{BET} , equals $614 \text{ m}^2/\text{g}$ which means that overall surface of the carbon cryogel/ceria composite, in comparison with the starting CC ($S_{BET} = 620 \text{ m}^2/\text{g}$), is almost the same, i.e. the presence of 10 wt.% of ceria did not change the S_{BET} . But, the median pore radius decreased from 14 nm to 7 nm (Table 1) due to the incorporation of the ceria particle into the porous structure of the carbon cryogel. By preparation of the composite sample in this way, the overall specific structure and mesoporosity of the material was preserved.

Presence of ceria has been examined by X-ray diffraction. X-ray diffraction patterns (Fig. 2) display diffraction peaks for the carbon cryogel/ceria composite. Diffraction peaks at 2θ values of 28° , 33° , 48° and 56° correspond to (111), (200), (220) and (222) planes of ceria, respectively [17]. Broad peaks with low intensity correspond to the diffraction profiles of the ceria structure superimposed on broaden profiles typical of carbon disordered structure [19]. The diffused profiles at 2θ values of 24° and 43° correspond to (002) and (10) reflections of a turbostratic carbon structure.

3.2. Adsorption kinetic study

Figure 3 (inset) shows adsorption kinetic of As(III) on the carbon cryogel/ceria composite. The arsenic removal rate was very fast and the adsorbed amount of As(III) increased gradually with time interval increment. Within the first 10 minutes over 93% of As(III) was removed. The equilibrium was reached after 2 h. Similar results have been reported in literature [20,21].

In order to evaluate the kinetic mechanism that controls an adsorption process, adsorption reaction models as well as adsorption diffusion models were applied to fit kinetic data [22]. The best-fit model was selected based on the values of the linear regression correlation coefficient, r^2 . Pseudo-second order kinetic model

Table 1. Porous properties of carbon cryogel/ceria composite

Sample	S_{BET} [m^2/g]	r_m [nm]	Reference
CC/ceria composite	614	7	this study
CC	620	14	[15]

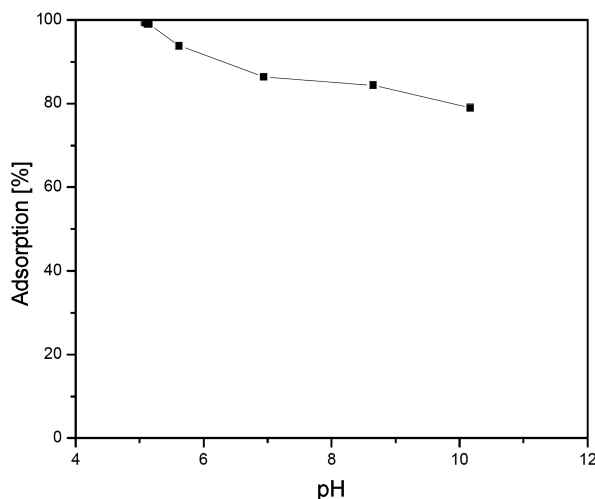


Figure 4. Percentage of As(III) adsorption on ceria/CC composite as a function of solution pH; $C_0 = 10 \text{ mg/l}$, $V = 25 \text{ ml}$, $m = 100 \text{ mg}$, $t = 24 \text{ h}$

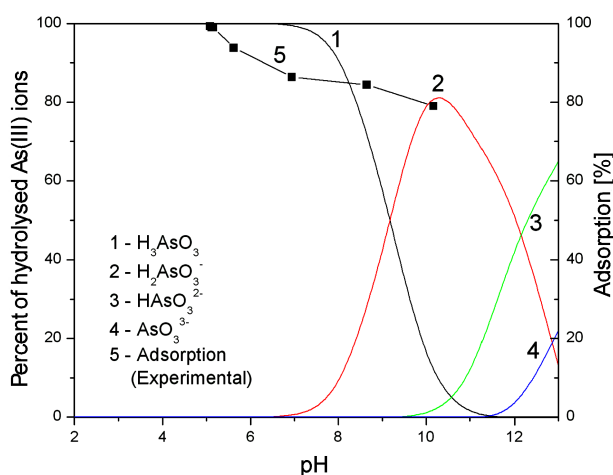


Figure 5. Comparison of the pH dependence of adsorbed As(III) ions percentage on carbon cryogel/ceria composite with the percentage of As(III) hydrolysis products; $C_0 = 10 \text{ mg/l}$, $V = 25 \text{ ml}$, $m = 100 \text{ mg}$, $t = 24 \text{ h}$

is represented by the equation (1) and its solution, equation (2), for $q = 0$ and $t = 0$:

$$\frac{dq}{dt} = k_2(q_e - q)^2 \quad (1)$$

$$\frac{t}{q} = \frac{1}{k_2 q_e^2} + \frac{1}{q_e} t \quad (2)$$

where k_2 is rate constant, t is time and q and q_e are transient and equilibrium amount of adsorbate, respectively. Relationship between t/q and t shows that experimental data, for the whole range of adsorption process, can be successfully correlated ($r^2 = 1$) by the pseudo-second order model (Fig. 3).

3.3. The effect of pH

Generally, the adsorption process is strongly affected by the solution pH. Figure 4 represents the percentage of

As(III) adsorption on the carbon cryogel/ceria composite as a function of solution pH. All results are presented as a function of final (equilibrium) solution pH since the amount of adsorbed ions depends on final pH. As it can be seen in Fig. 4, the amount of adsorbed As(III) ions is not strongly affected by the pH values. Namely, the maximum adsorption percentage is achieved at pH values below 5 and continually, slightly, decreases at higher pH values. This is in agreement with already reported literature data [20,21,23]. For the comparison, the adsorption percentage of As(III) ions on the pure CC did not show a significant difference at whole tested pH range, too. But, an increase of around 15% was recorded at pH 7–8 [15].

As in the case of the pure CC, the variation of solution pH value has an important effect on the interactions between arsenic and the adsorbent surface, because it affects the distribution of various hydrolysed arsenic species as well as the surface charge of adsorbent and should be discussed in view of different concentrations and forms of hydrolysed As(III) species and PZC (point of zero charge) of the carbon cryogel/ceria composite. Figure 5 shows the distribution of various hydrolysed As(III) species as a function of pH. The percentages of hydrolysis products were calculated from the equations and stability constants already presented in our previous paper [15].

By the comparison of the pH dependence of adsorbed As(III) ions percentage on the carbon cryogel/ceria composite with the percentage of As(III) hydrolysis products (Fig. 5) it can be concluded that hydrolysed As(III) ions were adsorbed as neutral molecule of arsenic acid (H_3AsO_3) and H_2AsO_3^- ions over the whole examined pH range (similarity between experimental and H_3AsO_3 (1) and H_2AsO_3^- (2) curves).

Additionally, we have already showed that hydrolysis of metal ions starts at lower pH values in presence of inorganic or organic species than in aqueous solutions [24]. In this case it means that, in the presence of the carbon cryogel/ceria composite, negatively charged H_2AsO_3^- ions exist at pH values lower than 7. On the other side, the surface charge of the adsorbent will influence the adsorption processes. Point of zero charge of the carbon cryogel/ceria composite was determined to be at pH around 7 (not shown here), i.e. positive charge develops on the composite surface at pH below 7, and the composite surface is negatively charged at pH above 7. Consequently, the adsorption percentage of negatively charged, hydrolysed, arsenic(III) ions will be higher below PZC.

Taking into account fact that main mechanism is adsorption of neutral molecules and that adsorption process is best fitted by the second-order kinetic model we can assume that rate determining step is diffusion process of the adsorbate within the pores of adsorbent.

The role of ceria on surface of the carbon cryogel/ceria composite could be twofold. Non-stoichiometric ceria reduces the amount of functional groups

and effects on correlated movements of electrons during the adsorbate-adsorbent interaction.

3.4. Adsorbent dose study

Prior the determination of adsorption isotherms, the optimal ratio between volume of the solution of As(III) ions and mass of the adsorbent was investigated. The constant volume of As(III) solutions is contacted with different masses of the composite material. The obtained results are presented in Fig. 6. The results are displayed as percentage of As(III) adsorption on the carbon cryogel/ceria vs. mass of the adsorbent. It is clear that with increasing of adsorbent mass the percentage of arsenic (III) adsorbed increases exponentially. According to these results, the optimal solution volume/mass of the adsorbent ratio was calculated (5 mg of adsorbent with 25 ml of the As(III) solution). By comparison with results obtained on the pure CC [15] (100 mg of adsorbent with 25 ml of the As(III) solution) the dose adsorbent is

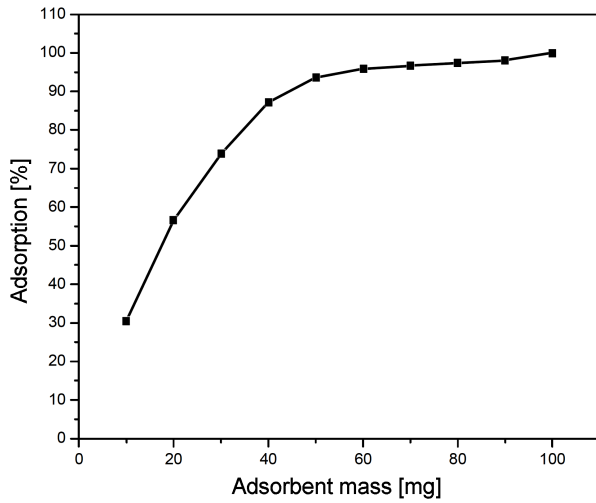


Figure 6. Percentage of As(III) adsorption on carbon cryogel/ceria composite as a function of adsorbent mass; $C_0 = 10 \text{ mg/l}$, $V = 25 \text{ ml}$, $t = 24 \text{ h}$, $\text{pH} = 5$

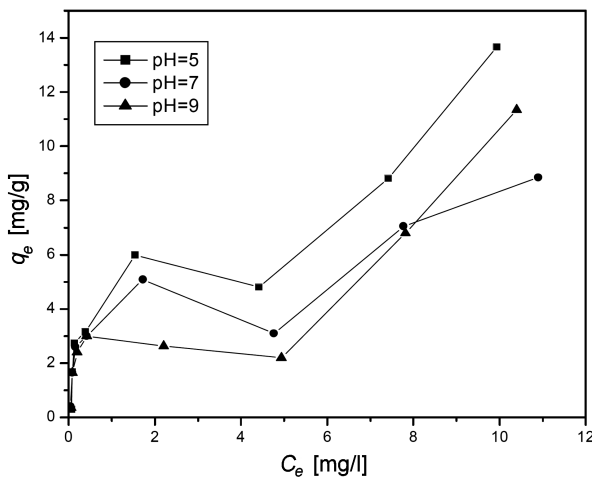


Figure 7. Adsorption isotherms for As(III) ions on carbon cryogel/ceria composite at different pH values; $C_0 = 0.25\text{-}14 \text{ mg/l}$, $V = 25 \text{ ml}$, $m = 5 \text{ mg}$, $t = 24 \text{ h}$

reduced 20 times, i.e. the sorption capacity of the carbon cryogel/ceria composite increased 20 times in comparison with CC.

3.5. Adsorption isotherms

Figure 7 shows adsorption isotherms for As(III) ions on the carbon cryogel/ceria composite at different pH values. The adsorption isotherms, presented in Fig. 7, confirmed our assumptions that adsorption is slightly pH dependent. Maximum adsorption capacity is achieved at $\text{pH} = 5$ which is in agreement with previous conclusions. Namely, according to the distribution diagram of the various hydrolysed As(III) species as a function of pH (Fig. 5), at $\text{pH} = 5$ As(III) is present only as a neutral molecule. Adsorption isotherms can be classified as A1 type [25,26]. The shape of isotherms shows that dispersion interactions are dominant in the adsorption of As(III) ions, which is characteristic of physical adsorption. Also, the shape of isotherms at higher equilibrium concentrations indicates the appearance of multilayer adsorption. Slight decrease of the adsorbed amount in pH region from 3 to 6 can be explained by changing of orientation and/or lateral interactions of adsorbed molecules.

Several isotherm models were used to interpret the equilibrium data. Among the few linear and non-linear models for fitting the adsorption isotherms [27] the BET isotherm for the modelling liquid phase adsorption shows the best agreement with experimental data [28]. The BET isotherm equation for liquid phase adsorption is:

$$q = q_m \frac{K_S C_{eq} [1 - (n+1)(K_L C_{eq})^n + n(K_L C_{eq})^{n+1}]}{(1 - K_L C_{eq}) [1 + (\frac{K_S}{K_L} - 1) K_L C_{eq} - (\frac{K_S}{K_L})(K_L C_{eq})^{n+1}]} \quad (3)$$

where: q is the amount of the adsorbate adsorbed on the solid surface, mg/g , q_m is the amount of the adsorbate corresponding to a complete monolayer adsorption, mg/g , C_{eq} is the equilibrium liquid phase concentration, mg/l , n is the maximum number of adsorbed layers on solid surface in BET isotherm, K_S is the equilibrium constant of adsorption for the 1st layer in BET isotherm, $(\text{mg/l})^{-1}$, and K_L is the equilibrium constant of adsorption for upper layers in the BET isotherm, $(\text{mg/l})^{-1}$.

For $n = \infty$:

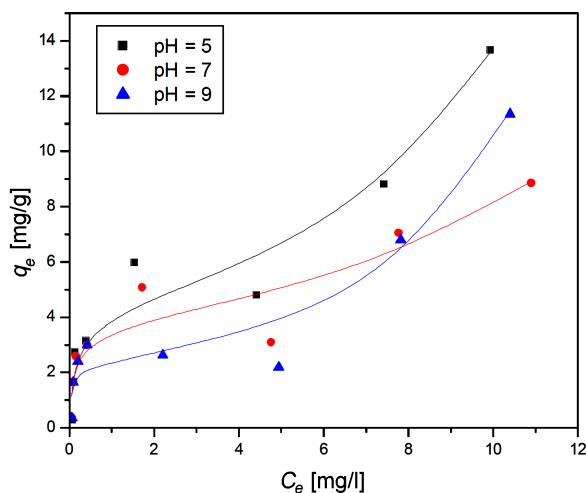
$$q = q_m \frac{K_S C_{eq}}{(1 - K_L C_{eq})(1 - K_L C_{eq} + K_S C_{eq})} \quad (4)$$

In the case of liquid phase adsorption the BET isotherm equation has three degrees of freedom (q_m , K_S , K_L) and it is impossible to convert this equation to a linear form and it can be solved by using nonlinear regression calculations.

As shown in Fig. 8, a good fit of the experimental data has been obtained (values for the coefficient of de-

Table 2. Values for q_m , K_S and K_L at different pH

	pH = 5	pH=7	pH=9
q_m [mg/g]	4.34	3.76	2.37
K_S [(mg/l) ⁻¹]	6.67	8.48	17.12
K_L [(mg/l) ⁻¹]	0.069	0.054	0.076
C_S [mg/l]	14.49	18.52	13.16
r^2	0.95	0.88	0.93

**Figure 8. Correlation of experimental data of adsorption of As(III) on carbon cryogel/ceria composite with BET isotherm for liquid phase adsorption (symbols – experimental data, line – BET equation)**

termination r^2 are presented in Table 2.). Values for the q_m , K_S and K_L , at different pH are presented in Table 2. According to the calculation, the amount of the adsorbate corresponding to the complete monolayer adsorption (q_m) decreases with increasing the pH of the solution. Also, equilibrium constant of adsorption for 1st layer (K_S) increases with increasing pH of the solution. Equilibrium constant of adsorption for upper layers (K_L) is changed with pH, too. In this model, the actual saturation concentration of liquid phase (C_S (mg/l)) is adjustable parameter and it is an inverse value of K_L . The large difference between calculated C_S values and value of saturation concentration of NaAsO_3 in aqueous solutions (156 g/100 ml) confirms that value for the saturation pressure in original BET equation for the gas phase could not be replaced with saturation concentrations of the adsorbate in the liquid phase.

IV. Conclusions

In order to improve the adsorption capacity of carbon cryogel, the carbon cryogel/ceria composite material with 10 wt.% of ceria was synthesized. Characterization by the FESEM showed that the homogeneous distribution of ceria on the surface of the carbon cryogel was achieved. Nitrogen adsorption confirmed that the high specific surface area and porous structure of the material were preserved. XRD analysis confirmed the presence of ceria. The adsorption process of As(III)

ions was investigated as a function of time, pH of the solution and adsorbate concentration. Adsorption kinetics followed the pseudo-second order model. Due to the hydrolysis, As(III) ions in water solutions are adsorbed as neutral molecules of H_3AsO_3 and consequently, the pH of the solution does not affect significantly the adsorption process. Based on these facts, it is assumed that rate-determining step in the adsorption process is diffusion of the adsorbate within the pores of adsorbent. Adsorption dose experiments, i.e. calculation of optimal ratio between the volume of the solution and mass of the adsorbent, showed that the mass of the adsorbent was reduced 20 times, in comparison with CC. The assumption is that presence of 10 wt.% of non-stoichiometric ceria reduced the amount of functional groups and influenced the correlated movements of electrons during the adsorbate-adsorbent interaction. Adsorption isotherms confirmed that the amount of As(III) removed is slightly pH-dependent and the shape of isotherms is characteristic for the physical, multilayer adsorption. Experimentally obtained isotherms are best-fitted by the application of BET isotherm for modeling the liquid phase adsorption.

Acknowledgements: This paper was supported by the Ministry of Science and Development, the Republic of Serbia, under Contract No. 45012.

References

1. L. Cheng-Che, Y. Hsin-Su, K. Ying-Chin, "Chronic arsenic exposure and its adverse health effects in Taiwan: A paradigm for management of a global environmental problem", *Kaohsiung J. Med. Sci.*, **27** (2011) 411–416.
2. R. Singh, S. Singh, P. Parihar, V.P. Singh, S.M. Prasad, "Arsenic contamination, consequences and remediation techniques: A review", *Ecotox. Environ. Safe.*, **112** (2015) 247–270.
3. D.G. Mazumder, U.B. Dasgupta, "Chronic arsenic toxicity: Studies in West Bengal, India", *Kaohsiung J. Med. Sci.*, **27** (2011) 360–370.
4. M. Yunus, N. Sohel, S.K. Hore, M. Rahman, "Arsenic exposure and adverse health effects: A review of recent findings from arsenic and health studies in Matlab, Bangladesh", *Kaohsiung J. Med. Sci.*, **27** (2011) 371–376.
5. D. Chakraborti, M.M. Rahman, M. Murrill, R. Das, Siddayya, S.G. Patil, A. Sarkar, H.J. Dadapeer, S. Yendigeri, R. Ahmed, K.K. Das, "Environmental arsenic contamination and its health effects in a historic gold mining area of the Mangalur greenstone belt of Northeastern Karnataka, India", *J. Hazard. Mater.*, **262** (2013) 1048–1055.
6. T.R. McClintock, Y. Chen, F. Parvez, D.V. Makarov, W. Ge, T. Islam, A. Ahmed, M. Rakibuz-Zaman, R. Hasas, G. Sarwar, V. Slavkovich, M.A. Bjurlin, J.H. Graziano, H. Ahsan, "Association between arsenic exposure from drinking water and hematuria: Re-

- sults from the health effects of arsenic, longitudinal study”, *Toxicol. Appl. Pharm.*, **276** (2014) 21–27.
7. K. Straif, L. Benbrahim-Tallaa, R. Baan, Y. Grosse, B. Secretan, F.E. Ghissassi, V. Bouvard, N. Guha, C. Freeman, L. Galichet, V. Coglianò, “A review of human carcinogens — Part C: metals, arsenic, dusts, and fibres”, *Lancet. Oncol.*, **10** (2009) 453–454.
 8. J.P. Lipps, A.S.C. Chen, S.E. McCall, L. Wang, *National Primary Drinking Water Regulations; Arsenic and Clarifications to Compliance and New Source Contaminants Monitoring Final Rule*: US EPA, Cincinnati, 2001.
 9. R. Yang, Y. Su, K.B. Aubrecht, X. Wang, H. Ma, R.B. Grubbs, B.S. Hsiao, B. Chu, “Thiol-functionalized chitin nanofibers for As (III) adsorption”, *Polymer*, **60** (2015) 9–17.
 10. M. Kanematsu, T.M. Young, K. Fukushima, P.G. Green, J.L. Darby, “Arsenic(III,V) adsorption on a goethite-based adsorbent in the presence of major co-existing ions: Modeling competitive adsorption consistent with spectroscopic and molecular evidence”, *Geochim. Cosmochim. Ac.*, **106** (2013) 404–428.
 11. M. Biterna, L. Antonoglou, E. Lazou, D. Voutsas, “Arsenite removal from waters by zero valent iron: Batch and column tests”, *Chemosphere*, **78** (2010) 7–12.
 12. H. Guo, Y. Li, K. Zhao, Y. Ren, C. Wei, “Removal of arsenite from water by synthetic siderite: Behaviors and mechanisms”, *J. Hazard. Mater.*, **186** (2011) 1847–1854.
 13. P.K. Dutta, A.K. Ray, V.K. Sharma, F.J. Millero, “Adsorption of arsenate and arsenite on titanium dioxide suspensions”, *J. Colloid. Interf. Sci.*, **278** (2004) 270–275.
 14. G. Ungureanu, S. Santos, R. Boaventura, C. Botelho, “Arsenic and antimony in water and wastewater: Overview of removal techniques with special reference to latest advances in adsorption”, *J. Environ. Manage.*, **151** (2015) 326–342.
 15. T.Z. Minović, J.J. Gulicovski, M.M. Stoiljković, B.M. Jokić, Lj.S. Živković, B.Z. Matović, B.M. Babić, “Surface characterization of mesoporous carbon cryogel and its application in arsenic (III) adsorption from aqueous solutions”, *Micropor. Mesopor. Mater.*, **201** (2015) 271–276.
 16. B. Babić, B. Kaluđerović, Lj. Vračar, N. Krstajić, “Characterization of carbon cryogel synthesized by sol-gel polycondensation and freeze-drying”, *Carbon*, **42** (2004) 2617–2624.
 17. B. Matović, J. Dukić, B. Babić, D. Bučevac, Z. Dohčević-Mitrović, M. Radović, S. Bošković, “Synthesis, calcination and characterization of nanosized ceria powders by self-propagating room temperature method”, *Ceram. Int.*, **39** (2013) 5007–5012.
 18. L.R. Radovic, C. Moreno-Castilla, J. Rivera-Utrilla, “Carbon materials as adsorbents in aqueous solutions” pp. 227–407 in *Chemistry and Physics of Carbon*. Edited by L.R. Radovic, Dekker, New York, 2001.
 19. G.M. Jenkins, K. Kawamura, *Polymeric Carbons: Carbon Fibre, Glass and Char*, Cambridge University Press, Cambridge, 1976.
 20. Z. He, S. Tian, P. Ning, “Adsorption of arsenate and arsenite from aqueous solutions by cerium-loaded cation exchange resin”, *J. Rare Earth*, **30** (2012) 563–572.
 21. R. Srivastava, “Eco-friendly and morphologically-controlled synthesis of porous CeO₂ microstructure and its application in water purification”, *J. Colloid. Interf. Sci.*, **348** (2010) 600–607.
 22. H. Qiu, L. Lv, B. Pan, Q. Zhang, W. Zhang, Q. Zhang, “Critical review in adsorption kinetic models”, *J. Zhejiang Univ. Sci. A*, **10** (2009) 716–724.
 23. X. Peng, Z. Luan, J. Ding, Z. Di, Y. Li, B. Tian, “Cerium nanoparticles supported on carbon nanotubes for the removal of arsenate from water”, *Mater. Lett.*, **59** (2005) 399–403.
 24. B.M. Babić, S.K. Milonjić, M.J. Polovina, S. Čupić, B.V. Kaluđerović, “Adsorption of zinc, cadmium and mercury ions from aqueous solutions on an activated carbon cloth”, *Carbon*, **40** (2002) 1109–1115.
 25. C.H. Giles, T.H. MacEwans, S.N. Nakhwa, D. Smith, “Studies in adsorption. Part XI. A system of classification of solution adsorption isotherms, and its use in diagnosis of adsorption mechanisms and in measurement of specific surface areas of solids”, *J. Chem. Soc.*, (1960) 3973–3993.
 26. C.H. Giles, D. Smith, A. Huitson, “A general treatment and classification of the solute adsorption isotherm. I. Theoretical”, *J. Colloid Interf. Sci.*, **47** (1974) 755–765.
 27. K.Y. Foo, B.H. Hameed, “Insights into the modeling of adsorption isotherm systems”, *Chem. Eng. J.*, **156** (2010) 2–10.
 28. A. Ebadi, J.S.S. Mohammadzadeh, A. Khudiev, “What is the correct form of BET isotherm for modeling liquid phase adsorption?”, *Adsorption*, **15** (2009) 65–73.

